J. Water Environ. Nanotechnol., 4(1): 40-47 Winter 2019

ORIGINAL RESEARCH PAPER

Removal of crystal violet using nanozeolite-x from aqueous solution: Central composite design optimization study

Siroos Shojaei[1,*], Jamal Ahmadi[2], Meysam Davoodabadi Farahani[3], Bentolhoda Mehdizadeh[4], Mohammadreza Pirkamali[1]

[1] *Young Researchers and Elite Club, Zahedan Branch, Islamic Azad University, Zahedan, Iran*
[2] *Department of Chemical Engineering, Amirkabir University of Technology, Tehran, Iran*
[3] *Faculty of mining, petroleum and geophysics engineering, Shahrood University of technology, Shahrood, Iran*
[4] *Department of Medical Engineering, Islamic Azad University, South Tehran Branch, Tehran, Iran*

Received: 2018-11-27 Accepted: 2019-01-06 Published: 2019-02-01

ABSTRACT

The remaining dye in the wastewater is not desirable as it damages the ecosystem and nature, and also is very toxic. The Crystal Violet (CV) dye is toxic and potentially carcinogenic. In addition, it reduces light in water and prevents the process of photosynthesis of aquatic plants. Therefore, nanozeolite-X (NX) was utilized as an adsorbent to remove the Crystal Violet (CV); effects of pH, catalyst mass, sonication time, and concentration of dye were also investigated. Effects of variables on the removal efficiency were studied via the Central Composite Design (CCD) to determine the dye removal percentage. The quadratic model was selected to predict the removal efficiency using the software. Optimal conditions for CV removal from aqueous solution were: pH= 8, sonication time= 6 min, concentration of dye= 13 mg L^{-1}, and catalyst mass= 0.26 g. In these circumstances, the recovery efficiency was 97.60%. The research results indicated that NX could be applied potentially for CV removal. .

Keywords: *Central Composite Design; Crystal Violet; Environmental; Experimental Design; Nanozeolite-X*

How to cite this article
Shojaei S, Ahmadi A, Davoodabadi Farahani M, Mehdizadeh B, Pirkamali MR. Removal of crystal violet using nanozeolite-x from aqueous solution: central composite design optimization study. J. Water Environ. Nanotechnol., 2019; 4(1): 40-47.
DOI: 10.22090/jwent.2019.01.004

INTRODUCTION

Dye is a central group of environmental pollutants and can be seen even by eyes. Therefore, the discharge of colored wastewater into water resources is strongly prohibited [1]. Sewage of factories and production centers complicates the wastewater treatment process due to various compounds [2]. Dyes are expressively crucial for some reasons such as reducing light penetration, affecting drinking water quality, causing allergies and skin irritation, genetic mutations, impairment in the process of photosynthesis, and carcinogenicity; hence, reducing and eliminating any types of dyes are significantly critical [3, 4]. Different methods have been proposed to remove dye from wastewater including coagulation and flocculation, chemical oxidation, membrane filtration, electrochemical purification, ion exchange, advanced oxidation, enzymatic decomposition, adsorption, electrochemical degradation and, photocatalyst use [5-10]. Among these techniques, the adsorption process has been more taken into account due to initial cost, simplicity and flexibility, easy operation, insensitivity to toxic compounds, the ability to remove organic and inorganic compounds such as dyestuffs and odoriferous compounds [11, 12]. Absorbent plays a key role in removing dye from wastewater. Today, research has focused on new adsorbents such as activated carbon, zeolite, sugar-beet pulp, and wheat shells that show high

* Corresponding Author Email: *shojaeisiroos@gmail.com*

absorption capacity [13-18]. Zeolites belong to the most prominent class of microporous materials that have many business applications [19]. It consists of elements of groups I and II of the periodic table (such as sodium and calcium), which enables zeolites to exchange cations. Zeolite crystals have been widely used because of micropore features, high thermal stability, low cost, high density, and adjustable composition[20, 21]. They have also been recently considered as potential adsorbents to remove dye from aqueous solutions. Zeolite has been reported to be used to remove anionic dyes from the environment. Alver and Metin observed that more than 93% adsorption was achieved using 0.25 g of adsorbent [22]. Bagheban Shahri et al [23]used 4A Zeolite as an adsorbent to remove the acridine orange dye. Optimum conditions were pH = 3.0, dye concentration 20.0 mg L^{-1}, time 80.0 min, and T = 298.0 K, with a maximum absorption of over 90% . Recent efforts to synthesize zeolites have increased their activity level and their ionic exchange properties. These nanocrystalline zeolites have a high potential for environmental catalysis, environmental modification, degradation and disposal of waste materials [21, 24-26]. One of the main goals of research is economic optimization. The classical methods of changing a variable at a time are time-consuming, they require a lot of experiments, and cannot show the interactive effects of the variables. Additionally, optimized process conditions using classical methods are not reliable. The empirical design technique enables researchers to logically reduce trials, reduce costs, and create more research interests. The response surface methodology (RSM) is a method for obtaining a desirable result to reduce the number of experiments and the interaction among beneficial factors reported by many researchers[27-29] . Thus, the present study aimed to optimize the process through the response surface methodology for removing Crystal violet dye by nanozeolite-X due to the relatively high efficiency of the process for removing various pollutants including dyestuffs.

EXPERIMENTAL

Chemical and Solutions

All reagents of analytical grade and deionized water were used throughout. Working standard solutions were prepared freshly at various concentrations by diluting the stock solution of dye (1000 mgL^{-1}). Table 1 presents the general characteristics of CV.

Characterization

Zeolite nanoparticles were characterized using X-Ray Diffraction (Siemens, D5000 with Cu Kα radiation) analysis. Scanning electron microscopy (KYKY-EM 3200) was used to analyze and understand the external surface of the adsorbent. Ultrasonic bath (KDC-200B Ultra Sonic System) at 40 kHz and 120 W power was used for ultrasound absorption.

Nanozeolite-X synthesis

NX was synthesized by a hydrothermal technique. Aluminosilicate gel containing 5.34 g of NaOH, 2.42 g of $NaAlO_2$, 3.43 g of SiO_2, and 50.0 g of H_2O was prepared in a plastic beaker weighing 250 ml. The final gel was transferred to the autoclave. Hydrothermal crystallization was carried out in a rotary shaker at 300 rpm at a temperature of 60 °C for 4 days. The product was rinsed with doubly distilled water (pH<8) and dried at 100 °C for 5 hours [30-32]. The NX was set and characterized using XRD and SEM.

Adsorption experiments

A batch procedure system was used for studies by NX as an adsorbent to remove CV dye from aqueous solutions. Tests were done in some test tubes (centrifuge tubes) (25 ml) containing various concentrations of CV (5-25 mg L^{-1}) and different values of NX (0.1-0.3 g). The solution was put in an ultrasonic bath for 2-10 minutes. The global buffer (HCl or NaOH 0.01 mol L^{-1}) was used to set pH (3-11). Finally, the solutions were centrifuged for three minutes. The CV concentration reduced over time due to the absorption of dye molecules on NX. Dye concentration was determined based on the obtained calibration curve at the maximum wavelength in the concentration range of performance. The dye removal efficiency was determined in different test conditions, discussed

Table 1. characteristics of the investigated dye.

Characteristic	
Color index name	Crystal Violet (CV)
Molecular formula	C25H30N3Cl
Molecular weight	407.98 (g mol^{-1})
λ_{max}	586 (nm)
Chemical structure	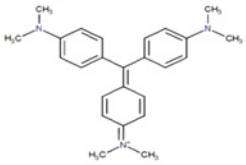

by the CCD method and optimized in the next section. The percentage of dye removal was calculated by Equation (1).

$$\text{Dye removal (\%)} = \frac{c_o - c_t}{c_o} \times 100 \quad (1)$$

In this equation, C_o is the initial concentration and C_t is the final concentration of dye in mg L^{-1}.

Empirical design: Response surface methodology (RSM)

RSM includes a group of mathematical and statistical techniques based on the proportionality of experimental models with obtained empirical data. Hence, linear or quadrilateral polynomial functions were utilized to describe the studied system, and then model test conditions until its optimization. Four independent variables were utilized to design CV removal tests. In the CCD, each variable was evaluated at 5 levels. Y refers to the predicted variance of design response, and X represents the selected independent variable points. The interaction between the above parameters can be converted into an equation in which these parameters and their coefficients are used to predict the optimal response for a set of experiments. Desirable conditions for the CV removal, by the tested adsorbent, were defined by the quadratic equation hat predicted the obtained model by the following formula:

$$y = \beta_0 + \sum_{i=1}^{4}\beta_i x_i + \sum_{i=1}^{4}\sum_{j=1}^{4}\beta_{ij} x_i x_j + \sum_{i=1}^{4}\beta_{ii} x_i^2 + \varepsilon \quad (2)$$

Where, y is the response; and β_0, β_i, and β_{ii} are regression coefficients of relevant variables to intercept linear and quadratic terms, respectively. X_i and X_j are independent variables, and ε is the remained equation. Statistical information was studied via the ANOVA (Analysis of variance) to justify the importance and adequacy of the model. The adequacy of response surface models was evaluated by calculating the coefficient of determination (R^2) as well as its test for the lack of fit. For the absorption process, important variables like pH, CV concentration, Catalyst mass, and sonication time were selected as independent variables. Conditions of the model were pH of 3 to 11, NX value of 0.1 to 0.3 g, sonication of 2 to 10 minutes, and CV concentration of 5 to 25 mg L^{-1} as presented in Table 2.

RESULTS AND DISCUSSION

Characterization of adsorbent

The SEM studied morphology and size of prepared NX particles. Nanocrystalline images of NX (Fig. 1a) indicate that particles had an approximate size of fewer than 100 nanometers and were agglomerated. The surface texture and morphology indicated a porous and rough surface of the adsorbent. This increased the effective surface for adsorption. Fig. 1b shows the sample XRD model of NX. The average sample size of 40-50 nm was obtained according to diffraction peaks at scales of 2°θ of 6°θ, 16°θ, 27°θ and also the Scherrer equation. Obviously, diffraction lines were extensively expanded and might indicate a smaller crystal size [33].

Model fitting and statistical analysis

In Table 2, CCD was selected with four independent variables namely pH, catalyst mass, sonication time, and concentration of dye at five levels for each. Table 3 presents 30 tests and their corresponding responses.

Table 4 presents the analysis of variance (ANOVA). ANOVA indicates that this model is significant through a high F-value (122.28), and there is only 0.01% of chance of noise (error). Meanwhile, a very low p-value ($p<0.0001$) also indicates that the selected model is very substantial. "R-squared" (0.9732) has a reasonable agreement with "Adj R-squared" (0.9642) providing a good prediction of the model. The quadratic empirical polynomial equation is obtained based on the ANOVA. It is as follows in terms of real factors:

y = +72.50 +6.67 Catalyst mass -5.00 Concentration of dye -5.67 Sonication time +3.92 pH +0.13 Catalyst mass* Concentration of dye +0.13 Catalyst mass* Sonication time -0.12 Catalyst mass* pH -0.12 Concentration of dye* Sonication time

Table 2. Experimental range and levels of independent process variables.

Variables	Unit	Levels				
Catalyst mass	g	0.1	0.15	0.2	0.25	0. 3
Concentration of dye	mgL^{-1}	5	10	15	20	25
Sonication time	min	2	4	6	8	10
pH	----	3	5	7	9	11

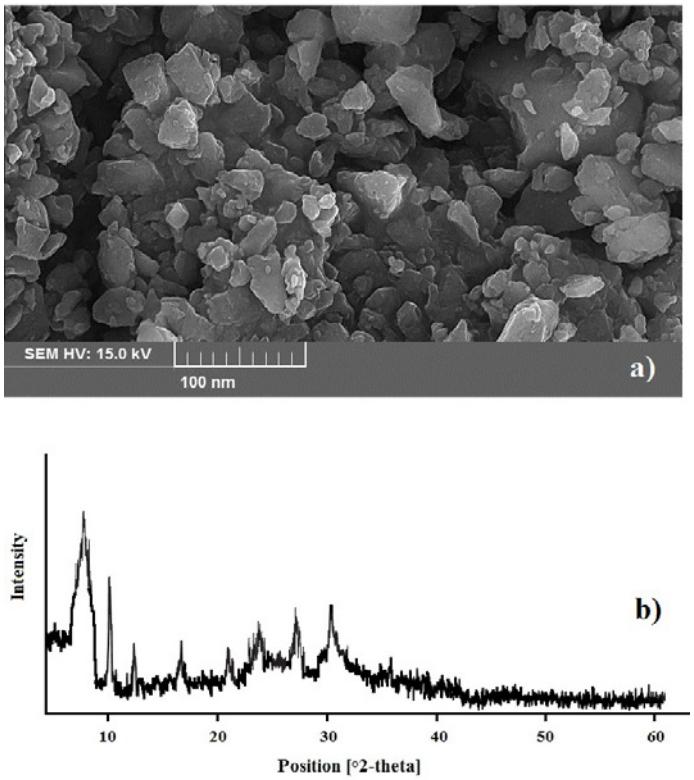

Fig. 1. a) The SEM image of NX. b) XRD pattern of NX.

Table 3. Result of central composite design.

Run	Catalyst mass (g)	Concentration of dye (mg L^{-1})	Sonication time (min)	pH	Dye removal (%)	
					Experimental	Predicted
1	0.20	15	10	7	64.34	64.18
2	0.15	20	4	5	66.76	67.67
3	0.30	15	6	7	90.51	91.06
4	0.25	20	4	5	79.75	79.01
5	0.20	15	6	7	72.69	72.29
6	0.15	20	8	5	55.83	54. 94
7	0.15	10	4	9	84.96	85.00
8	0.20	25	6	7	63.42	92.98
9	0.20	5	6	7	84.77	84.23
10	0.25	20	8	9	76.83	75.99
11	0.15	20	8	9	63.45	63.15
12	0.20	15	6	7	74.21	74.87
13	0.25	10	4	9	95.68	95.88
14	0.25	10	8	5	78.79	79.31
15	0.20	15	6	3	66.50	66.24
16	0.15	20	4	9	74.66	74.02
17	0.25	10	8	9	86.34	86.41
18	0.15	10	4	5	76.94	77.13
19	0.20	15	6	7	74.62	73.86
20	0.25	20	4	9	87.46	87.91
21	0.20	15	6	11	82.57	81.73
22	0.20	15	6	7	72.34	73.06
23	0.20	15	6	7	73.04	72.75
24	0.15	10	8	5	65.69	66.31
25	0.10	15	6	7	61.96	62.28
26	0.20	15	2	7	89.74	88.49
27	0.15	10	8	9	73.67	74.10
28	0.25	20	8	5	68.34	67.84
29	0.25	10	4	5	89.94	89.21
30	0.20	15	6	7	73.60	74.26

+0.13 Concentration of dye, pH +0.13 Sonication time, pH +0.92 (Catalyst mass)^2 +0.42

(Concentration of dye)^2 +1.17 (Sonication time)^2 +0.54(pH)^2 (3)

Where, y is the percentage removal of CV (%).

Fig.2(a) displays the actual and predicted percentage of CV removal. Based on this chart, the calculated values correspond to experimental values, and there is a satisfactory correlation between these values using the second-order prediction model.

Three-dimensional response surface plots

Fig.2(b-d) shows response surface plots of the removal percentage and the interaction between variables. The three-dimensional response surface plots are organized based on a quadratic model. The plots indicate the relative effect of two variables on the adsorption efficiency, while all other variables are at constant levels.Fig.2 (b) illustrates the effects of catalyst mass and dye concentration (variables) on the CV removal. According to this plot, an increase in the catalyst mass enhances the efficiency of CV removal as the more the catalyst mass is increased, the more active sites of catalyst are available leading to the increased percentage of dye removal [34]. The removal percentage is also reduced by declining the color concentration because the ratio of dye molecules to catalyst is low at lower dye concentrations; thus, most dye molecules stick on the surface of the catalyst, and they are removed from the solution leading to a rise in CV removal percentage [29]. Fig.2 (c) shows the interaction of catalyst mass and pH variables. CV dye is a cationic dye that has a positive charge in its structure. Therefore, in acidic pH, various functional groups, both in the dye and in the absorbent structures are positively charged. This creates a strong repulsion force between the dye and the absorbent surface, which significantly reduces the percentage of CV removal. PH = 8 is close to neutral pH, which is a very important advantage

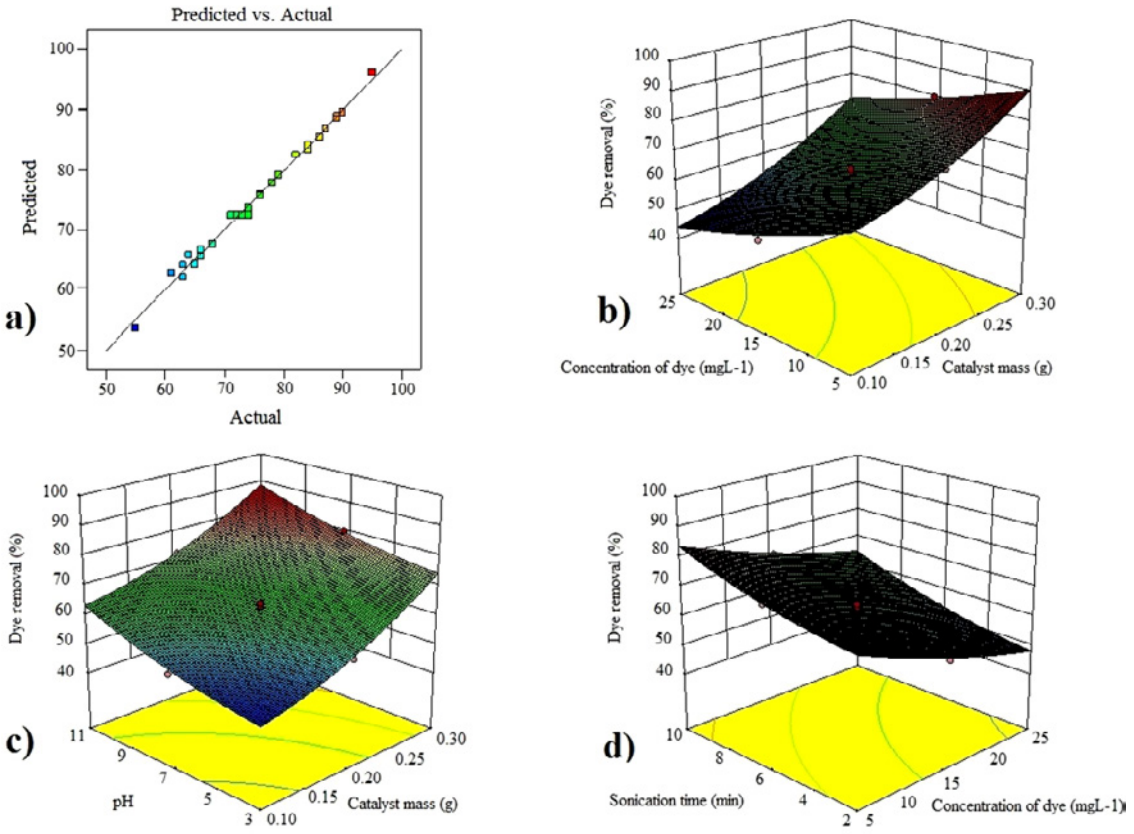

Fig.2 a) The actual and predicted response plot of CV removal b) The combined effect of catalyst mass and concentration of dye c) The combined effect of catalyst mass and pH d) The combined effect of concentration of dye and sonication time on CV removal.

Table 4. Analysis of variance (ANOVA) results of the quadratic model.

Source	Sum of square	Mean square	F-value	P-value	Remarks
Model	2862.78	204.48	122.28	< 0.0001	Significant
A-Catalyst dosage	1066.67	1066.67	637.87	< 0.0001	
B-Dye concentration	600.00	600.00	358.80	< 0.0001``	
C- pH	770.67	770.67	460.86	< 0.0001	
D- Time	368.17	368.17	220.17	< 0.0001	
AB	0.25	0.25	0.15	0.7044	
AC	0.25	0.25	0.15	0.7044	
AD	0.25	0.25	0.15	0.7044	
BC	0.25	0.25	0.15	0.7044	
BD	0.25	0.25	0.15	0.7044	
CD	0.25	0.25	0.15	0.7044	
A^2	23.05	23.05	13.78	0.0021	
B^2	4.76	4.76	2.85	0.1122	
C^2	37.33	37.33	22.33	0.0003	
D^2	8.05	8.05	4.81	0.0444	
Residual	25.08	1.67			
Lack of Fit	15.58	1.56	0.82	0.6320	Not-significant

R^2= 0. 9732, Adj-R^2= 0.9642

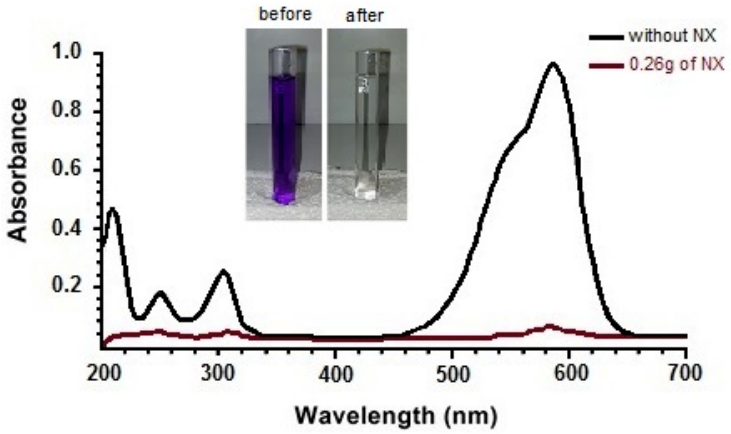

Fig. 3. UV–vis absorbance spectra of decomposed CV solution over NX. The inset shows the photos of dye solutions before and after adsorption. (sonication time 6min, catalyst mass 0.26 g, pH of solution 8, concentration of dye 13 mg L^{-1}).

to remove this dye [35]. Fig. 2(d) displays response surface plots of the dye removal as dependent on dye concentration and sonication time. A rise in the sonication time increases the opportunity for interaction of catalyst and dye molecules leasing to the removal of more molecules from dye plus increasing the percentage of dye removal [36].

Optimization of Reaction

Three solutions with different values of ideal conditions (with reported mean) were used to predict optimal conditions for CV removal to find the most effective factors in this process in order to validate the predicted model and optimize variables. The optimization modeling process suggested the optimal values of various process variables (pH= 8, sonication time= 6 min, dye concentration= 13 mg L^{-1}, and catalyst mass= 0.26 g) to achieve the maximum removal (97.60%) of CV dye from aqueous solution. The relationship between the adsorbent amount and removal efficiency was investigated in the next series of experiments. As shown in Fig. 3, we saw a decrease in the peak absorption at 586 nm with increasing NX. The ability to remove the dye was also shown by changing the dye of the solutions in the absence and presence of NX (Inset in Fig. 3). This change in dyes shows that NX can completely absorb CV.

CONCLUSIONS

Results of the present research indicated that NX was an efficient adsorbent to remove CV. Experiments were done as a function of pH, sonication time, concentration of dye, and catalyst

mass, which were fully studied and optimized. The quadratic model was designed to predict the removal efficiency of CV and then was analyzed by the ANOVA. ANOVA results (R^2= 97.32%, F-value (very high), and P-value<0.0001) indicated that a quadratic model was suitable for the empirical data. Optimized values of pH= 8, sonication time= 6 min, concentration of dye= 13 mg L^{-1}, and catalyst mass= 0.26 g were finally obtained. The maximum removal was 97.60% according to optimal conditions.

ACKNOWLEDGEMENTS

The authors are grateful to University of Payame Noor, for kind support.

CONFLICT OF INTEREST

The authors declare that they have no competing interests.

REFERENCES

1. Chieng HI, Lim LBL, Priyantha N. Enhancing adsorption capacity of toxic malachite green dye through chemically modified breadnut peel: equilibrium, thermodynamics, kinetics and regeneration studies. Environmental Technology. 2014;36(1):86-97.
2. Akcil A, Erust C, Ozdemiroglu S, Fonti V, Beolchini F. A review of approaches and techniques used in aquatic contaminated sediments: metal removal and stabilization by chemical and biotechnological processes. Journal of Cleaner Production. 2015;86:24-36.
3. Shojaei, S., et al., Removal of Reactive Red 198 by Nanoparticle Zero Valent Iron in the Presence of Hydrogen Peroxide. Journal of Water and Environmental Nanotechnology, 2017. 2(2): p. 129-135.
4. Carneiro PA, Umbuzeiro GA, Oliveira DP, Zanoni MVB. Assessment of water contamination caused by a mutagenic textile effluent/dyehouse effluent bearing disperse dyes. Journal of Hazardous Materials. 2010;174(1-3):694-9.
5. Shojaei S, Shojaei S, Sasani M. The efficiency of eliminating Direct Red 81 by Zero- valent Iron nanoparticles from aqueous solutions using response surface Model (RSM). Modeling Earth Systems and Environment. 2017;3(1).
6. Chidambaram T, Oren Y, Noel M. Fouling of nanofiltration membranes by dyes during brine recovery from textile dye bath wastewater. Chemical Engineering Journal. 2015;262:156-68.
7. Santos SCR, Boaventura RAR. Treatment of a simulated textile wastewater in a sequencing batch reactor (SBR) with addition of a low-cost adsorbent. Journal of Hazardous Materials. 2015;291:74-82.
8. Panda KK, Mathews AP. Ozone oxidation kinetics of Reactive Blue 19 anthraquinone dye in a tubular in situ ozone generator and reactor: Modeling and sensitivity analyses. Chemical Engineering Journal. 2014;255:553-67.
9. Eren, Z., Ultrasound as a basic and auxiliary process for dye remediation: A review. Journal of Environmental Management, 2012. 104: p. 127-141.
10. Robinson T, McMullan G, Marchant R, Nigam P. Remediation of dyes in textile effluent: a critical review on current treatment technologies with a proposed alternative. Bioresource Technology. 2001;77(3):247-55.
11. Greluk M, Hubicki Z. Efficient removal of Acid Orange 7 dye from water using the strongly basic anion exchange resin Amberlite IRA-958. Desalination. 2011;278(1-3):219-26.
12. Zhao C, Deng H, Li Y, Liu Z. Photodegradation of oxytetracycline in aqueous by 5A and 13X loaded with TiO2 under UV irradiation. Journal of Hazardous Materials. 2010;176(1-3):884-92.
13. Aksu Z, Isoglu IA. Use of agricultural waste sugar beet pulp for the removal of Gemazol turquoise blue-G reactive dye from aqueous solution. Journal of Hazardous Materials. 2006;137(1):418-30.
14. Gupta VK, Jain R, Varshney S. Removal of Reactofix golden yellow 3 RFN from aqueous solution using wheat husk—An agricultural waste. Journal of Hazardous Materials. 2007;142(1-2):443-8.
15. Lorencgrabowska E, Gryglewicz G. Adsorption characteristics of Congo Red on coal-based mesoporous activated carbon. Dyes and Pigments. 2007;74(1):34-40.
16. Shojaei S, Shojaei S, Pirkamali M. Application of Box–Behnken Design Approach for Removal of Acid Black 26 from Aqueous Solution Using Zeolite: Modeling, Optimization, and Study of Interactive Variables. Water Conservation Science and Engineering. 2019.
17. Faki Ae, Turan M, Ozdemir O, Turan AZ. Analysis of Fixed-Bed Column Adsorption of Reactive Yellow 176 onto Surfactant-Modified Zeolite. Industrial & Engineering Chemistry Research. 2008;47(18):6999-7004.
18. Jain R, Gupta VK, Sikarwar S. Adsorption and desorption studies on hazardous dye Naphthol Yellow S. Journal of Hazardous Materials. 2010;182(1-3):749-56.
19. Yang RT. Adsorbents: Fundamentals and Applications: John Wiley & Sons, Inc.; 2003 2003/04/18.
20. Li C, Dong Y, Wu D, Peng L, Kong H. Surfactant modified zeolite as adsorbent for removal of humic acid from water. Applied Clay Science. 2011;52(4):353-7.
21. Ahmaruzzaman M. A review on the utilization of fly ash. Progress in Energy and Combustion Science. 2010;36(3):327-63.
22. Alver E, Metin AÜ. Anionic dye removal from aqueous solutions using modified zeolite: Adsorption kinetics and isotherm studies. Chemical Engineering Journal. 2012;200-202:59-67.
23. Bagheban Shahri F, Niazi A, Akrami A. Application of Full Factorial Design for Removal of Polycyclic Aromatic Dye from Aqueous Solution Using 4A Zeolite: Adsorption Isotherms, Thermodynamic and Kinetic Studies. Polycyclic Aromatic Compounds. 2016;38(2):141-56.
24. Larsen SC. Nanocrystalline Zeolites and Zeolite Structures: Synthesis, Characterization, and Applications. The Journal of Physical Chemistry C. 2007;111(50):18464-74.
25. Modhera B, Chakraborty M, Parikh PA, Jasra RV. Synthesis of nano-crystalline zeolite β: Effects of crystallization parameters. Crystal Research and Technology. 2009;44(4):379-85.
26. Gross-Lorgouilloux M, Caullet P, Soulard M, Patarin J, Moleiro E, Saude I. Conversion of coal fly ashes into faujasite under soft temperature and pressure conditions.

Mechanisms of crystallisation. Microporous and Mesoporous Materials. 2010;131(1-3):407-17.
27. Tan IAW, Ahmad AL, Hameed BH. Preparation of activated carbon from coconut husk: Optimization study on removal of 2,4,6-trichlorophenol using response surface methodology. Journal of Hazardous Materials. 2008;153(1-2):709-17.
28. Kumar SNA, Ritesh SK, Sharmila G, Muthukumaran C. Extraction optimization and characterization of water soluble red purple pigment from floral bracts of Bougainvillea glabra. Arabian Journal of Chemistry. 2017;10:S2145-S50.
29. Shojaei S, Shojaei S. Optimization of process variables by the application of response surface methodology for dye removal using nanoscale zero-valent iron. International Journal of Environmental Science and Technology. 2018.
30. Wang H, Holmberg BA, Yan Y. Synthesis of Template-Free Zeolite Nanocrystals by Using in Situ Thermoreversible Polymer Hydrogels. Journal of the American Chemical Society. 2003;125(33):9928-9.
31. Wang H, Wang Z, Yan Y. Colloidal suspensions of template-removed zeolite nanocrystals. Chemical Communications. 2000(23):2333-4.
32. Jakubinek MB, Zhan B-Z, White MA. Temperature-dependent thermal conductivity of powdered zeolite NaX. Microporous and Mesoporous Materials. 2007;103(1-3):108-12.
33. Oh W-C, Jung A-R, Ko W-B. Characterization and relative photonic efficiencies of a new nanocarbon/TiO2 composite photocatalyst designed for organic dye decomposition and bactericidal activity. Materials Science and Engineering: C. 2009;29(4):1338-47.
34. Dutta S, Saha R, Kalita H, Bezbaruah AN. Rapid reductive degradation of azo and anthraquinone dyes by nanoscale zero-valent iron. Environmental Technology & Innovation. 2016;5:176-87.
35. Shojaei S, Shojaei S. Experimental design and modeling of removal of Acid Green 25 dye by nanoscale zero-valent iron. Euro-Mediterranean Journal for Environmental Integration. 2017;2(1).
36. Fan J, Guo Y, Wang J, Fan M. Rapid decolorization of azo dye methyl orange in aqueous solution by nanoscale zerovalent iron particles. Journal of Hazardous Materials. 2009;166(2-3):904-10.